Atmos. Chem. Phys., 10, 9863–9878, 2010
www.atmos-chem-phys.net/10/9863/2010/
doi:10.5194/acp-10-9863-2010

Atmospheric Chemistry and Physics

Improved global modelling of HO_x recycling in isoprene oxidation: evaluation against the GABRIEL and INTEX-A aircraft campaign measurements

T. Stavrakou[1], **J. Peeters**[2], **and J.-F. Müller**[1]

[1]Belgian Institute for Space Aeronomy, Avenue Circulaire 3, 1180, Brussels, Belgium
[2]Katholieke Universiteit Leuven, Celestijnenlaan 200F, 3001, Leuven, Belgium

Received: 22 June 2010 – Published in Atmos. Chem. Phys. Discuss.: 2 July 2010
Revised: 28 September 2010 – Accepted: 7 October 2010 – Published: 19 October 2010

Abstract. Stimulated by recent important developments regarding the oxidation chemistry of isoprene, this study evaluates and quantifies the impacts of different mechanism updates on the boundary layer concentrations of OH and HO_2 radicals using the IMAGESv2 global chemistry transport model. The model results for HO_x, isoprene, NO, and ozone are evaluated against air-based observations from the GABRIEL campaign, conducted over the Guyanas in October 2005, and from the INTEX-A campaign over the Eastern US in summer 2004. The version 2 of the Mainz Isoprene Mechanism (MIM2, Taraborrelli et al., 2009) used as reference mechanism in our simulations, has been modified to test (i) the artificial OH recycling proposed by Lelieveld et al. (2008), (ii) the epoxide formation mechanism proposed by Paulot et al. (2009b), and finally (iii) the HO_x regeneration of the Leuven Isoprene Mechanism (LIM0) proposed by Peeters et al. (2009); Peeters and Müller (2010). The simulations show that the LIM0 scheme holds by far the largest potential impact on HO_x concentrations over densely vegetated areas in the Tropics as well as at mid-latitudes. Strong increases, by up to a factor of 4 in the modelled OH concentrations, and by a factor of 2.5–3 in the HO_2 abundances are estimated through the LIM0 mechanism compared to the traditional isoprene degradation schemes. Comparatively much smaller OH increases (<25%) are associated with the implementation of the mechanism of Paulot et al. (2009b); moreover, the global production of epoxides is strongly suppressed (by a factor of 4) when the LIM0 scheme is combined with this mechanism. Hydroperoxy-aldehydes (HPALDs) are found to be major first-generation products in the oxidation of isoprene by OH, with a combined globally averaged yield of 50–60%. The use of the LIM0 chemistry in the global model allows for reconciling the model with the observed concentrations at a satisfactory level, compared to the other tested mechanisms, as the observed averaged mixing ratios of both OH and HO_2 in the boundary layer can be reproduced to within 30%. In spite of the remaining uncertainties in the theoretically-predicted rates of critical radical reactions leading to the formation of HPALDs, and even more in the subsequent degradation of these new compounds, the current findings make a strong case for the newly proposed chemical scheme. Experimental confirmation and quantification is urgently needed for the formation of HPALDs and for their fast OH-generating photolysis.

Correspondence to: T. Stavrakou
(jenny@aeronomie.be)

1 Introduction

A large body of recent literature studies provides overwhelming evidence that the isoprene oxidation mechanisms used in chemistry-transport models require substantial revision. These mechanisms adopted consensus pathways based on first-generation product data acquired in laboratory experiments at very high NO levels (0.5 to 10 ppmv, Atkinson et al., 2006) duly complemented by peroxy + HO_2 routes recognized to be competing with the peroxy + NO reactions at atmospheric NO levels. However, different studies, based on comparisons between aircraft campaign and in situ measurements and models, point

towards the existence of a currently unaccounted production mechanism that could explain the high abundances of the OH and HO_2 radicals observed in remote, isoprene-rich environments (Kuhn et al., 2007; Kubistin et al., 2008; Lelieveld et al., 2008; Butler et al., 2008; Martinez et al., 2010), but also over rural or even suburban regions with strong biogenic influence and moderate NO_x levels (Tan et al., 2001; Ren et al., 2008; Hofzumahaus et al., 2009).

A strong OH regeneration, through the reactions of isoprene peroxy radicals with HO_2, was invoked in an attempt to explain the high observed HO_x levels during the GABRIEL airborne campaign over Suriname (Lelieveld et al., 2008). Although this hypothesis allows for a better agreement between the models and the observations of the GABRIEL campaign (Butler et al., 2008), no experimental evidence for OH formation via the reactions of saturated analogues of isoprene peroxys with HO_2 has been observed, in contrast with the cases of acyl peroxy and 2-oxo-peroxy radical reaction with HO_2 (Dillon and Crowley, 2008). In a recent laboratory study, Paulot et al. (2009b) showed that the OH-reaction of isoprene hydroperoxides regenerates OH along with dihydroxy epoxides, highly soluble compounds possibly involved in secondary organic aerosol formation from isoprene degradation.

A promising explanation for the gap between modelled and observed HO_x abundances might be provided by the theoretical study of Peeters et al. (2009), which showed that isomerization reactions of specific isomer/conformer peroxy radicals from isoprene lead to the formation of HO_x radicals and photolabile hydroperoxy-aldehydes (denoted HPALDs), at rates such that the traditional reactions of the isoprene peroxy radicals (with NO and HO_2) are outrun in most non-urban atmospheric conditions. Besides this direct OH formation, HPALDs are also believed to hold a high potential for additional OH-(photo)production, as argued by Peeters and Müller (2010). Based on recent observations by Paulot et al. (2009b) and Karl et al. (2009), relatively minor adjustments were brought to the mechanism (Peeters and Müller, 2010). These adaptations, however, leave intact the large expected implications for the oxidizing capacity of the atmosphere, especially under low NO and high isoprene levels.

The aim of this study is to quantify the impact of the aforementioned newly proposed mechanistic changes in the isoprene degradation on the global tropospheric composition. To this purpose, the IMAGESv2 global chemistry-transport model (Stavrakou et al., 2009) is employed and one-year-long simulations are performed using different isoprene degradation schemes. The manuscript is organized as follows. In Sect. 2, we describe the isoprene + OH reaction schemes and how they are implemented in the global model. We start with the Mainz Isoprene Mechanism (MIM2, Taraborrelli et al., 2009), which serves as the base scheme for our simulations, as well as the MIM2+ scheme (Lelieveld et al., 2008), and we continue with the epoxide formation mechanism (Paulot et al., 2009b) and the Leuven Isoprene Mechanism (LIM0, Peeters et al., 2009) including the rate and mechanism adjustments proposed in Peeters and Müller (2010) (Sect. 2.2 and 2.3). A brief description of the global model is provided in Sect. 2.4. In Sect. 3 the impacts of the mechanistic changes are quantified and the predicted concentrations of OH, HO_2, isoprene, NO, and ozone are evaluated against measurement campaigns over the Amazon basin (GABRIEL, Lelieveld et al., 2008) and over the Eastern United States (INTEX-A, Ren et al., 2008). Conclusions are drawn in Sect. 4.

2 Isoprene reaction schemes in a global model

This section presents the different isoprene degradation mechanisms tested with the global model. The model simulations are summarized in Table 2. The Mainz Isoprene Mechanism (MIM2) and its version MIM2+ are presented in Subsect. 2.1, the new pathways proposed by Paulot et al. (2009b) and Peeters et al. (2009) are presented in Subsect. 2.2 and Subsect. 2.3, respectively. Finally, a brief description of the IMAGESv2 model is provided in Subsect. 2.4.

2.1 The MIM2 and MIM2+ isoprene schemes

Our basis mechanism is a modified version of the MIM2 mechanism (Taraborrelli et al., 2009), itself a reduction of the detailed Master Chemical Mechanism (MCMv3.1, Jenkin et al., 1997; Saunders et al., 2003). MIM2 and MCM consider OH addition to the terminal carbons, while neglecting the minor addition to the inner carbons. Subsequent O_2-addition results in two β-hydroxyperoxy radicals, ISOPBO2 and ISOPDO2 and two δ-hydroxyperoxy radicals, ISOPAO2 and ISOPCO2 in MCM, lumped into a single compound in MIM2, LISOPACO2 (see Table 1):

$$\mathrm{ISOP} + \mathrm{OH} \rightarrow 0.25\,\mathrm{LISOPACO2} + 0.491\,\mathrm{ISOPBO2} + 0.259\,\mathrm{ISOPDO2}. \quad (1)$$

The MIM2 version used here includes the modifications discussed in Taraborrelli et al. (2009), and in particular, the OH-forming channel in the reactions of HO_2 with acyl peroxy radicals and with 2-oxo peroxy radicals, with branching ratios of 0.5 and 0.15, respectively, based on laboratory investigations (Dillon and Crowley, 2008; Jenkin et al., 2008).

Following Butler et al. (2008) (also Pugh et al., 2010a), we reduce by 50% the effective rate constant of isoprene + OH, relative to the IUPAC recommended rate (Atkinson et al., 2006). This reduction, which was found necessary in the context of model comparisons with measurements of HO_x and isoprene in the boundary layer over Amazonia (Butler et al., 2008) and Borneo (Pugh et al., 2010a), is tentatively justified by the inefficient mixing of isoprene, leading to a segregation of isoprene and OH (Krol et al., 2000). The use of a unique value for the rate reduction cannot but be a very

Table 1. Abbreviated name and chemical formula (Lewis structure) of isoprene degradation products appearing in this article.

Abbreviated name	Chemical formula
	C_5 hydroxyperoxy radicals
LISOPACO2	$HOCH_2-C(CH_3)=CH-CH_2O_2\bullet$
	$\bullet O_2CH_2-C(CH_3)=CH-CH_2OH$
ISOPBO2	$HOCH_2-C(CH_3)(O_2\bullet)-CH=CH_2$
ISOPDO2	$CH_2=C(CH_3)-CH(O_2\bullet)-CH_2OH$
ISOPEO2	$\bullet O_2CH_2-C(CH_3)(OH)-CH=CH_2$
	$CH_2=C(CH_3)-CH(OH)-CH_2O_2\bullet$
	C_5 hydroxy hydroperoxides
LISOPACOOH	$HOCH_2-C(CH_3)=CH-CH_2OOH$
	$HOOCH_2-C(CH_3)=CHCH_2OH$
ISOPBOOH	$HOCH_2-C(CH_3)(OOH)-CH=CH_2$
ISOPDOOH	$CH_2=C(CH_3)-CH(OOH)-CH_2OH$
ISOPEOOH	$HOOCH_2-C(CH_3)(OH)-CH=CH_2$
	$CH_2=C(CH_3)-CH(OH)-CH_2OOH$
	C_4-C_5 carbonyls
HPALD1	$OCH-C(CH_3)=CH-CH_2OOH$
HPALD2	$OCH-CH=C(CH_3)-CH_2OOH$
HALD51	$HOCH_2-CH=C(CH_3)-CHO$
HALD52	$HOCH_2-C(CH_3)=CH-CHO$
HALD4	$CH_2=C(CH_2OH)-CHO$
MACR	$CH_2=C(CH_3)-CHO$
MVK	$CH_3-C(O)-CH=CH_2$
HCOC5	$CH_2=C(CH_3)-C(O)-CH_2OH$
	Epoxides
IEPOX	$HOCH_2-\overline{CHOC(CH_3)}-CH_2OH$

crude approximation, since the segregation intensity is determined by the local spatio-temporal heterogeneity in the emissions and by the competition between two very heterogeneous processes, namely mixing and chemical destruction. Moreover, a recent analysis of high-frequency isoprene measurements above the tropical rainforest in Borneo suggests a much weaker segregation intensity than the one applied here, with a rate reduction factor of the order of 0.9 (Pugh et al., 2010b). The effect of the OH-isoprene rate reduction will be estimated in a sensitivity comparison with the global model (S6 vs. S5, Table 2).

In addition, we account for the possible regeneration of HO_x in the OH-oxidation of glycolaldehyde (GLYALD) and hydroxyacetone (HYAC), by adopting the product distribution observed at low O_2 and low NO in the laboratory studies of Butkovskaya et al. (2006a) and Butkovskaya et al. (2006b), respectively:

$$\begin{aligned}\mathrm{GLYALD+OH} \rightarrow\ & 0.25\,\mathrm{OH}+0.75\,\mathrm{HO_2} \\ & +0.17\,\mathrm{GLY}+0.17\,\mathrm{HCOOH} \\ & +0.67\,\mathrm{HCHO}+0.5\,\mathrm{CO}+0.34\,\mathrm{CO_2},\end{aligned} \quad (2)$$

$$\begin{aligned}\mathrm{HYAC+OH} \rightarrow\ & 0.1\,\mathrm{OH}+0.825\,\mathrm{HO_2} \\ & +0.75\,\mathrm{MGLY}+0.125\,\mathrm{HCOOH} \\ & +0.125\,\mathrm{CH3O_2}+0.125\,\mathrm{CH3COOH} \\ & +0.05\,\mathrm{CO}+0.2\,\mathrm{CO_2}.\end{aligned} \quad (3)$$

Here GLY and MGLY stand for glyoxal and methylglyoxal, respectively. Finally, the products of the OH-reaction of methylglyoxal are updated according to Baeza-Romero et al. (2007):

$$\begin{aligned}\mathrm{MGLY+OH} \rightarrow\ & 0.6\,\mathrm{CH_3CO_3}+0.4\,\mathrm{CH_3O_2} \\ & +\mathrm{CO}+\mathrm{H_2O}.\end{aligned} \quad (4)$$

The resulting mechanism will be utilized in the standard S0 simulation. Modifications to this mechanism will be tested throughout a series of sensitivity tests (Table 2), so as to evaluate the impact of recent findings related to isoprene degradation.

In the S1 simulation, the OH-forming channel in the reactions of acyl peroxy and 2-oxo peroxy radicals is neglected. In the S2 case, the standard mechanism is modified with the artificial addition of two OH radicals formed in the reactions of HO_2 with all isoprene peroxy radicals (MIM2+), as proposed by Lelieveld et al. (2008) and extensively discussed by Butler et al. (2008).

2.2 Epoxide formation following Paulot et al. (2009b)

The impact of epoxide formation as proposed by Paulot et al. (2009b) is investigated in the S3 scenario. These compounds are formed under low-NO_x conditions, in the OH-oxidation of the isoprene hydroxy-hydroperoxides, themselves formed from the reaction of the isoprene peroxy radicals with HO_2. Epoxide formation is accompanied by OH regeneration and is implemented in the model as shown below:

$$\mathrm{LISOPACOOH+OH} \rightarrow \mathrm{IEPOX+OH} \quad (5)$$

$$\mathrm{ISOPBOOH+OH} \rightarrow \mathrm{IEPOX+OH} \quad (6)$$

$$\begin{aligned}\mathrm{ISOPBOOH+OH} \rightarrow\ & 0.7\,\mathrm{ISOPBO2} \\ & +0.3\,\mathrm{HCOC5}+0.3\,\mathrm{OH}.\end{aligned} \quad (7)$$

Similar reactions apply for ISOPDOOH. The adopted reaction rates are (in $\mathrm{cm^3\,molec^{-1}\,s^{-1}}$) 1.07×10^{-10}, $1.9\times10^{-11}\exp(390/T)$, and $0.38\times10^{-11}\exp(200/T)$, respectively. HCOC5 is a C_5 aldehyde in the MCMv3.1 mechanism. Based on Paulot et al. (2009b), the subsequent oxidation of IEPOX is written as follows:

Table 2. Simulations performed using the IMAGESv2 global model.

Simulation	Description
S0	standard, modified MIM2 chemistry, effective C_5H_8 + OH reaction rate set equal to 50% of the IUPAC rate
S1	as S0, without OH-forming channel in RO_2 + HO_2 reactions
S2	as S0, addition of 2 OH radicals formed in the HO_2 reaction of isoprene peroxy radicals (Lelieveld et al., 2008) (MIM2+)
S3	as S0, with formation of epoxides and OH-regeneration in the ROOH + OH reactions following Paulot et al. (2009b)
S4	as S3, with LIM0 chemistry (Peeters et al., 2009; Peeters and Müller, 2010) and generation of 1 OH + 1 HO_2 in photolysis of HPALDs
S5	as S4, generation of 3 OH + 1 HO_2 in photolysis of HPALDs
S6	as S5, effective rate for C_5H_8 + OH reaction taken equal to 90% of the IUPAC rate
S7	as S6, with halved rate for the 1,6-H shift of Z-δ hydroxyperoxy radicals from isoprene
S8	as S7, with isoprene emissions halved over the US, and increased by 50% over the Guyanas

$$\mathrm{IEPOX} + \mathrm{OH} \rightarrow \mathrm{IEPOXO2} \quad (8)$$

$$\mathrm{IEPOXO2} + \mathrm{NO} \rightarrow \mathrm{IEPOXO} + \mathrm{NO_2} \quad (9)$$

$$\mathrm{IEPOXO2} + \mathrm{HO_2} \rightarrow \mathrm{IEPOXO} + \mathrm{OH} + \mathrm{O_2}, \quad (10)$$

with

$$\begin{aligned}\mathrm{IEPOXO} \rightarrow\ & 0.725\,\mathrm{HYAC} + 0.275\,\mathrm{GLY} \\ & + 0.275\,\mathrm{GLYALD} + 0.275\,\mathrm{MGLY} \\ & + 0.375\,\mathrm{HCHO} + 0.074\,\mathrm{HCOOH} \\ & + 0.125\,\mathrm{OH} + 0.825\,\mathrm{HO_2} + 0.251\,\mathrm{CO}.\end{aligned} \quad (11)$$

Note that the assumption of a unique, radical-propagating channel in the reaction of IEPOXO2 with HO_2 (reaction 10) is most probably unrealistic, and that a hydroperoxide should instead be formed in high yield. Its further oxidation as well as the fate of the oxy radical IEPOXO (reaction 11) will require more attention in future investigations.

2.3 The Leuven Isoprene Mechanism LIM0 (Peeters et al., 2009; Peeters and Müller, 2010)

New, theoretically proposed, pathways in the OH-initiated oxidation mechanism of isoprene (version 0 of the LIM mechanism, Peeters et al., 2009; Peeters and Müller, 2010) are implemented in simulations S4–S8. The main findings of this scheme are summarized below (see also Fig. 1).

1. The isoprene hydroxyperoxy radicals can eliminate O_2 – at rates of 1–10 s^{-1} at 303 K (green arrows on Fig. 1) – so that the various isomers/conformers can rapidly interconvert via O_2 re-addition, resulting in near-equilibrium steady-state populations (except at very high NO levels, >200 ppbv). The δ-OH-peroxys being by far less stable than the β-OH peroxys, the formation of hydroxy-aldehydes (HALDs) and other products from their reactions with NO, HO_2 and other RO_2 is hampered at NO concentrations lower that 1 ppbv. As pointed out by Peeters and Müller (2010), this explains the non-detection of the HALDs in atmospheric conditions and in laboratory experiments conducted at moderate NO levels.

2. The β-peroxys may undergo 1,5-H shifts (in light blue on Fig. 1), leading to OH and HCHO production along with either methacrolein (MACR) or methylvinylketone (MVK). Following Peeters and Müller (2010), the 1,5-H shift rates are adjusted in order to match the yield of MACR + MVK (12%) measured by Paulot et al. (2009b) in their OH-isoprene oxidation experiments conducted in near-absence of NO_x. Though it was recently argued that a fair share of the MVK + MACR in the Paulot et al. (2009b) experiments may result from permutation reactions of the isoprene-peroxy radicals (Archibald et al., 2010), Paulot et al. (2009b) invoked fairly fast 1,5-H shift reactions and the

sizeable coincident production of ^{16}OH also to explain the unexpected rapid appearance of isotopically light ISOPOOH hydroperoxides ($m/z = 203$) in their ^{18}OH- and H^{18}O^{18}O- labeled experiments. Although the issue of the MVK + MACR source(s) in these experiments is not definitely resolved, we follow the reasoning of Paulot et al. (2009b) in this for the time being. Thus, the adopted rates are equal to five times the geometric average of the rates estimated by Peeters et al. (2009): $k(1,5) = 4.81 \times 10^{11} \exp(-9203/T)\ \mathrm{s}^{-1}$.

3. The Z-δ-OH-peroxys can undergo fast 1,6-H shifts (in red in Fig. 1) leading, upon reaction with O_2, to the formation of HO_2 and hydroperoxy aldehydes (HPALDs). Following Peeters and Müller (2010), since the large difference (factor of 8) between the theoretically predicted rates for the two Z-δ-OH peroxys is very probably artificial, and as it might lead to unrealistically high MVK/MACR ratios in atmospheric conditions (Karl et al., 2009; Karl, 2010; Archibald et al., 2010), we adopt the geometric average of the rates estimates by Peeters et al. (2009): $k(1,6) = 8.48 \times 10^{8} \exp(-5930/T)\ \mathrm{s}^{-1}$. The uncertainty range for this crucial (averaged) rate is estimated by Peeters and Müller (2010) to be between 0.3 and 1.3 times this adopted value, based on two independent experimental constraints: the observed yield of MVK and MACR in the OH-initiated isoprene oxidation experiments of Karl et al. (2006) conducted at moderate NO levels, and the peroxy radical budget in the experiments of Paulot et al. (2009b). In addition, Archibald et al. (2010) concluded from box model simulations of the experiments by Paulot et al. (2009b) that the 1,6-H shift rates estimated from first principles by Peeters et al. (2009) should be both equalised and reduced to some extent in order to match the observations, in particular for the formation rate of hydroperoxides.

4. The HPALDs photodissociate rapidly, due to the combination of their highly absorptive conjugated carbonyl chromophore and very weak O-OH bond:

$$\mathrm{HPALD} + h\nu(+2\mathrm{O_2}) \rightarrow \mathrm{OH} + \mathrm{HO_2} + \mathrm{PACALDs}, \quad (12)$$

where the PACALDs are peroxy-acid-aldehydes. The photolysis rates are calculated by using the absorption cross section of MACR (Sander et al., 2006) and a unity quantum yield as argued in Peeters and Müller (2010). The PACALDs photolyse even more rapidly than the HPALDs, producing OH and a peroxy radical that will eventually yield an extra OH (Peeters and Müller, 2010). Therefore, the photolysis of HPALDs is expected to yield between 1 and 3 OH radicals. Moreover, all channels in the OH-reaction of HPALDs are expected to regenerate OH. The reactions of PACALDs with OH are negligibly slow compared to photolysis.

In the S4 simulation, we modify the S3 chemical mechanism to include the proposed updates of the LIM0 mechanism. The reaction of isoprene with OH is written as

$$\begin{aligned}\mathrm{ISOP} + \mathrm{OH} \rightarrow\ & 0.6\,\mathrm{ISOPBO2} + 0.3\,\mathrm{ISOPDO2} \\ & + 0.1\,\mathrm{ISOPEO2},\end{aligned} \quad (13)$$

where ISOPBO2 and ISOPDO2 represent the peroxys formed through OH-addition to the terminal carbons (Fig. 1), whereas ISOPEO2 represents the peroxys formed through the remaining minor additions. The δ-hydroxy peroxy radicals (LISOPACO2) are omitted, since their traditional reaction products have negligible yields in most atmospheric conditions. The OH-addition branching ratios follow the structure-activity relationship of Peeters et al. (2007). Note that an even lower branching ratio ($7 \pm 3\%$) for addition to the central carbons has been deduced in the experimental studies of Park et al. (2004). Moreover, Greenwald et al. (2010) theoretically predicted that at least one of the central OH-adducts should react with O_2 to yield HO_2 and 4-penten-2-one for a large fraction.

We account for the isomerization of the isoprene hydroperoxys through the following reactions:

$$\mathrm{ISOPBO2} \rightarrow \mathrm{HPALD1} + \mathrm{HO_2} \quad (14)$$

$$\mathrm{ISOPBO2} \rightarrow \mathrm{MVK} + \mathrm{HCHO} + \mathrm{OH} \quad (15)$$

$$\mathrm{ISOPDO2} \rightarrow \mathrm{HPALD2} + \mathrm{HO_2} \quad (16)$$

$$\mathrm{ISOPDO2} \rightarrow \mathrm{MACR} + \mathrm{HCHO} + \mathrm{OH}, \quad (17)$$

whereas their reaction rates (in s^{-1}):

$$k_{14} = 4.06 \times 10^{9} \exp(-7302/T) \quad (18)$$

$$k_{15} = k_{17} = 2.08 \times 10^{11} \exp(-8993/T) \quad (19)$$

$$k_{16} = 8.5 \times 10^{9} \exp(-7432/T) \quad (20)$$

were adjusted so that the yields of key compounds in the simplified scheme are the same as those of the explicit mechanism shown on Fig. 1. The reactions of ISOPBO2 and ISOPDO2 with NO and HO_2 are obtained from the MIM2 mechanism (Taraborrelli et al., 2009). The cross reactions of the isoprene peroxy radicals are also taken into account, based on experimental self-reaction rates for structurally similar peroxy radicals (Peeters and Müller, 2010).

The photolysis of the HPALDs is represented as

$$\begin{aligned}\mathrm{HPALD1} + h\nu \rightarrow\ & m\,\mathrm{OH} + \mathrm{HO_2} + 0.5\,\mathrm{HYAC} \\ & + 0.5\,\mathrm{MGLY} + 0.5\,\mathrm{GLYALD} + \mathrm{HCHO}\end{aligned} \quad (21)$$

$$\begin{aligned}\mathrm{HPALD2} + h\nu \rightarrow\ & m\,\mathrm{OH} + \mathrm{HO_2} + 0.5\,\mathrm{HYAC} \\ & + 0.5\,\mathrm{GLY} + 0.5\,\mathrm{GLYALD} + \mathrm{HCHO}\end{aligned} \quad (22)$$

where the value of the parameter m is set to either 1 or 3 (S4 and S5), to account for the extra OH radicals produced in

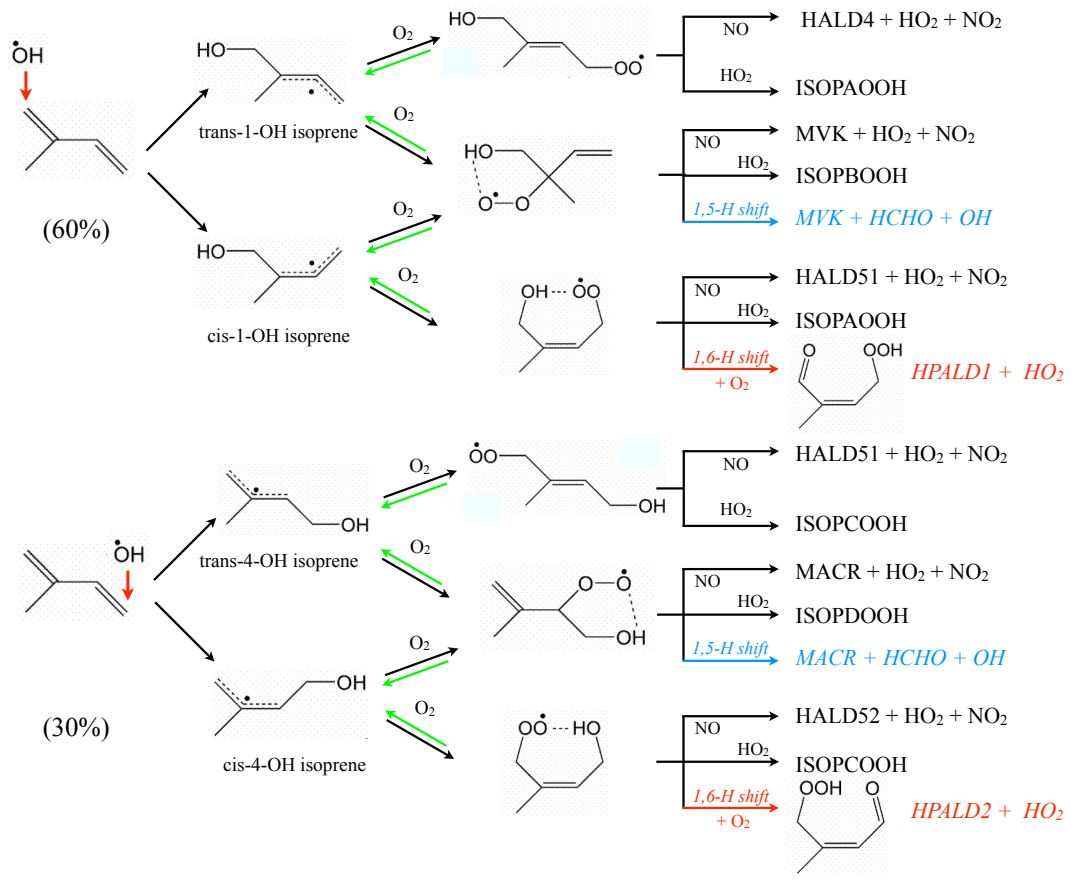

Fig. 1. Reaction scheme for OH addition to isoprene following Peeters et al. (2009). The minor addition channels (inner carbons 2 and 3) are not shown. HALD4, HALD51 and HALD52 are the C_4 and C_5 hydroxy-aldehydes formed in the NO-reaction of the δ-hydroxyperoxys (see Park et al. (2004) and references therein).

the photolysis of PACALDs (Eq. 12), as reported in Peeters and Müller (2010). The other formed compounds are typical isoprene oxidation products very likely to be generated in the photooxidation of the HPALDs.

The S6 scenario investigates how the choice for the isoprene + OH effective rate value impacts the model predictions. The effective rate of the isoprene + OH reaction is assumed to be equal to 90% of the IUPAC rate in this simulation. Further, in the S7 simulation, we explore the impact of a factor of two reduction in the 1,6-H shift of the Z-δ hydroxyperoxy radicals, in line with the estimated uncertainty range and possible overestimation of these rates suggested by experimental data (see above). In this case, the reaction rates of the reduced LIM0 scheme (reactions 14–17) become (in s^{-1})

$$k_{14} = 1.203 \times 10^9 \exp(-7127/T) \quad (23)$$

$$k_{15} = k_{17} = 2.04 \times 10^{11} \exp(-8987/T) \quad (24)$$

$$k_{16} = 1.571 \times 10^9 \exp(-7098/T). \quad (25)$$

2.4 IMAGESv2 brief description

The latest version of the global tropospheric chemistry-transport model IMAGESv2 is used in this study (Müller and Stavrakou, 2005; Stavrakou et al., 2009). The model is run at a horizontal resolution of $2° \times 2.5°$ and is discretized on 40 vertical levels from the surface up to the pressure of 44 hPa. The model calculates the concentrations of 128 chemical compounds with a 4-month spin-up starting on 1st September 2004. Simulations are performed for the year 2005. Transport is driven by monthly averaged ERA-Interim meteorological fields, whereas daily fields are used for water vapour, temperature, cloud optical depths, updraft mass fluxes, convective and stratiform precipitation fluxes, and boundary layer heights. The diurnal variations of the concentrations are calculated from a full diurnal cycle simulation using a 20-min timestep and the forth order Rosenbrock solver of the Kinetic Preprocessor (Sandu et al., 2006). Anthropogenic emissions are as in Stavrakou et al. (2009a). Monthly biomass burning emissions are obtained from the Global Fire Emissions Database (GFED) version 2 (van der Werf et al., 2006) for the year of the

simulation. Isoprene emissions are obtained from an updated version of the MEGAN-ECMWF inventory (Müller et al., 2008), which is driven by ERA-Interim meteorological fields, instead of operational ECMWF analyses as in Müller et al. (2008). It covers the period from 1997 to 2009 and is fully accessible at the MEGAN-ECMWF website (http://tropo.aeronomie.be/models/mohycan.htm). The global annual isoprene emissions for 2005 are estimated to 428 Tg/yr.

Dry deposition is computed using a resistance-in-series model based on Wesely (1989). Typical daily averaged deposition velocities over forested areas range between 0.6 and 1 cm s^{-1} for carbonyls and organic nitrates from isoprene, and between 1.3 and 1.7 cm s^{-1} for isoprene hydroperoxides and epoxides. Note that substantially higher deposition velocities of MACR and MVK have been reported, based on field campaign measurements over tropical forests (Karl et al., 2004; Kuhn et al., 2007). These high values should significantly depress the calculated near-surface concentrations of these compounds, with however only limited impacts on their global budget, given the dominance of the OH-reaction over deposition losses. The wet scavenging parameterization has been thoroughly described in the Supplement of Stavrakou et al. (2009a). For isoprene hydroperoxides and epoxides, the Henry's Law coefficient of hydroxy methyl hydroperoxide is used ($1.24 \times 10^{-8} \exp(9700/T)$ mol l^{-1} atm^{-1}, Sander, 1999). For the isoprene hydroxy nitrates, we use the average value for three $C_{>3}$ hydroxy nitrates (Sander, 1999), $1.32 \times 10^{-10} \exp(9433/T)$. MACR and MVK are considered non-soluble. Wet and dry deposition of the HPALDs are neglected, owing to their very short photochemical lifetimes.

3 Results

3.1 Impacts of mechanistic updates

We present in this section the impacts of the different mechanism updates (Table 2) on the OH and HO_2 concentrations in the boundary layer calculated with the IMAGESv2 model. The results for the month of July are shown on Figs. 2, 3, and 4. The global annual production of key compounds in the isoprene degradation mechanism, as well as the global isoprene + OH sink calculated for each simulation are summarized in Table 3.

Among all tested mechanism updates, the LIM0 mechanism achieves the largest HO_x concentration increase, when assuming $m = 3$ (S5 simulation, Fig. 4). The PBL-averaged OH concentration increases in S5 reach a factor of 2.5–3 over tropical forests, and a factor of 1.3–2 over the southeastern US compared to the S3 simulation. Lower but significant increases are calculated over Europe and boreal forests. Similar enhancements are found for HO_2 concentrations, with somewhat lower values. As a result of the enhanced OH concentrations, the global isoprene sink due to OH-reaction in S5 is estimated to be 12% higher compared to the S3 case. Archibald et al. (2010) also reported large increases (up to a factor of 3) in the OH concentrations after implementation of the Peeters et al. (2009) mechanism among other mechanistic changes in a box modelling study performed under low NO_x conditions. Nonetheless, their reported changes in the surface OH concentrations over the Amazon inferred from global model simulations turn out to be much weaker (factor of up to 1.4). A possible explanation for this discrepancy is the strongly overestimated NO_x concentrations calculated by the STOCHEM global model over Amazonia compared to measured values from the GABRIEL campaign (Lelieveld et al., 2008; Butler et al., 2008). Moreover, the photolysis of the HPALDs has been assumed to produce one OH radical in Archibald et al. (2010), whereas, in our simulations, one HO_2 and one to three OH radicals can be formed. Finally, whereas the OH-oxidation of HPALDs regenerates OH in LIM0, the strict application of the MCM protocol assumed in Archibald et al. (2010) probably leads to a net OH sink.

As a consequence of the large OH regeneration of the LIM0 chemistry, the OH concentrations in the boundary layer become only weakly sensitive to isoprene emissions, as illustrated on Fig. 6. Whereas a 10% increase in isoprene emissions leads to OH decreases reaching up to -10% over remote areas when the MIM2 mechanism is used (S0), the corresponding OH concentration decrease does not exceed −3% when the LIM0 chemistry is used (S5).

The major difference between the results of S4/S5 simulations and those of simulations S0–S3 is the formation of HPALDs, which accounts for the largest part (ca. 60% on a molar basis) of the isoprene sink by OH oxidation. Even when reducing the reaction rate of the 1,6-H shift reaction by a factor of two (S7), the yield of HPALDs remains very large, 50% globally, demonstrating the robustness of the impacts calculated in this study. Note that the higher effective rate for the isoprene + OH reaction assumed in S6/S7 has only little effect on the averaged product yields (Table 3) and on the HO_x levels, but obviously causes substantial decreases in isoprene mixing ratios. Logically, whereas the HPALD yield is found to exceed 50% in most regions, lower values (25–50%) are calculated over more polluted areas, such as Western Europe (Peeters and Müller, 2010).

Another important consequence of the LIM0 mechanism is the low global production of MVK and MACR, due to the fast 1,6-H shift pathways leading to the HPALDs, whereas the 1,5-H shift reactions leading to MVK and MACR (Fig. 1) are comparatively slower. More specifically, the globally averaged yield of MACR + MVK, 37% in the S3 case, is reduced to only 20% in S5 and S6 (28% in S7), half of it being due to the 1,5-H shift pathways, the remainder to the traditional reactions. Note that the larger yield of MVK in S0 compared to S3 is due to the 100% regeneration of ISOPBO2 in the MIM2 reaction of ISOPBOOH with OH, which artificially increases the concentration of ISOPBO2, and therefore the yield of MVK produced from its reaction with NO.

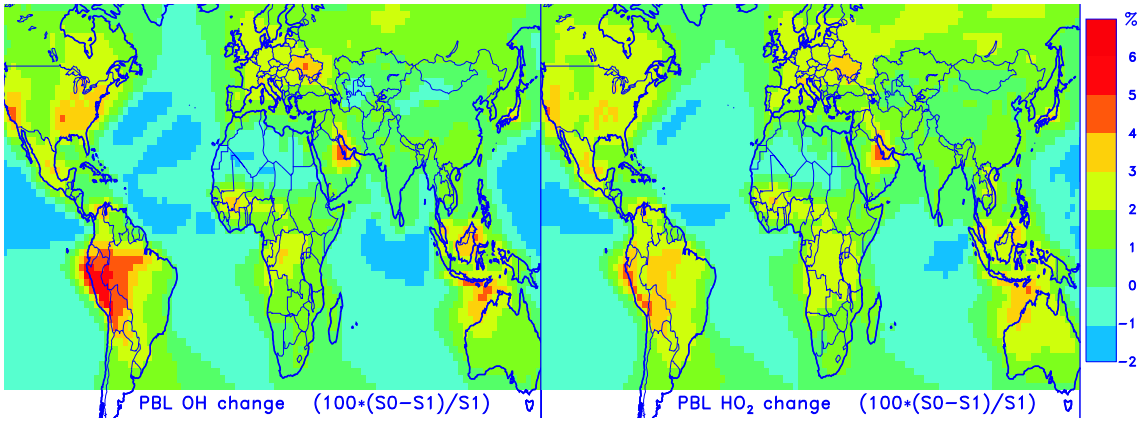

Fig. 2. Calculated percentage change in OH (left) and HO_2 (right) concentrations below 1.5 km altitude in July 2005 due to the inclusion of the OH-forming channel in specific $RO_2 + HO_2$ reactions.

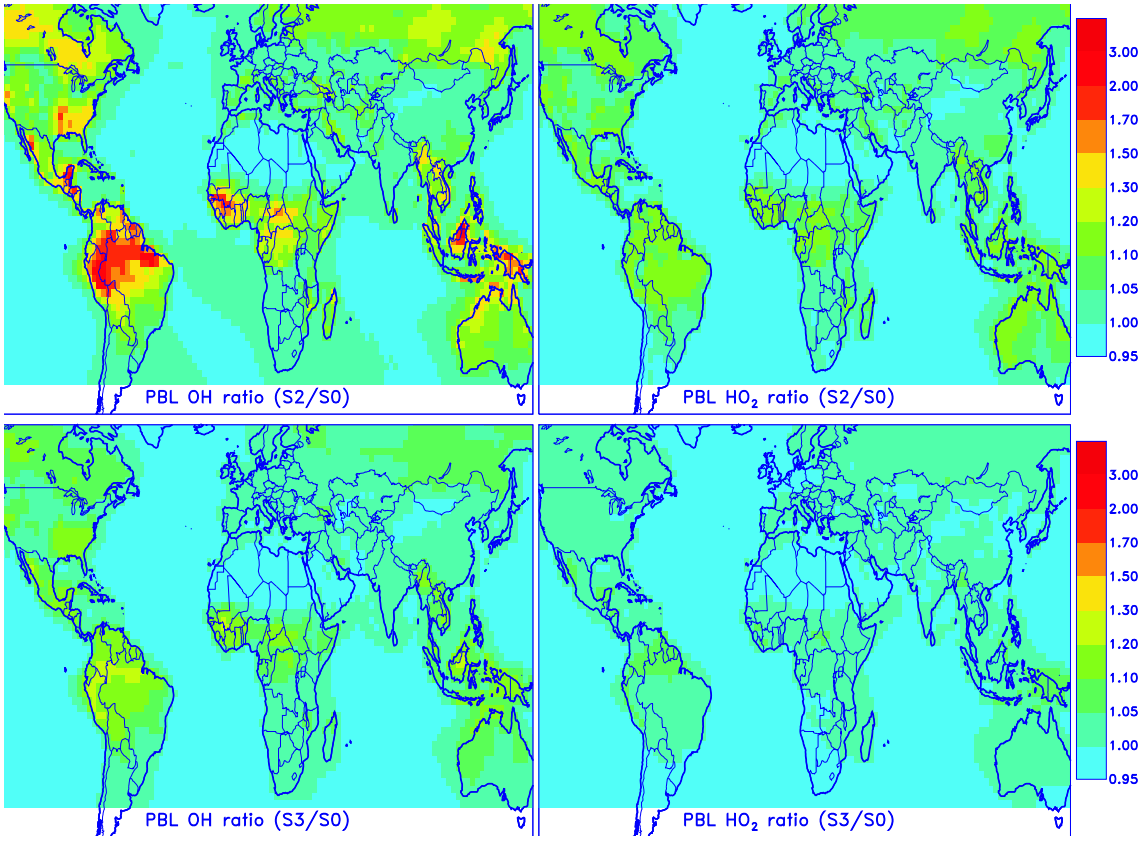

Fig. 3. Calculated impact on OH (left) and HO_2 (right) concentrations (July 2005, below 1.5 km) of (1) the artificial addition of 2 OH radicals formed in the reaction of isoprene peroxy radicals with HO_2 (upper panels), and (2) the epoxide formation and oxidation mechanism (lower panels).

An additional feature of the simulations S4 and S5 with respect to S0–S3 is the strong reduction of the isoprene nitrate production, estimated at less than 1% of the global isoprene sink from OH-oxidation, about ten times lower than in S0–S3 results. This reduction is due, on the one hand, to the fast interconversion of the isoprene hydroxy peroxys which strongly depresses the population of the δ-hydroxy peroxy radicals (LISOPACO2 in MIM2) characterized by high assumed nitrate yields upon reaction with NO (24%, Paulot et al., 2009a), and on the other hand, to the competition of the NO-reaction with the fast isomerizations (14–17) and with the enhanced HO_2-reaction.

Table 3. Calculated annual isoprene + OH sink and global production of major by-products from the isoprene + OH reaction: MVK and MACR (not including their production from isoprene + O_3), hydroperoxides (LISOPACOOH, ISOPBOOH, ISOPDOOH, ISOPEOOH), isoprene nitrates (LISOPACNO3, ISOPBNO3, and ISOPDNO3), epoxides (IEPOX), and hydroperoxy-aldehydes (HPALDs) for the simulations described in Table 2. Numbers are in Tmole yr^{-1}.

Simulation	S0	S1	S2	S3	S4	S5	S6	S7
Isoprene + OH sink	4.75	4.72	5.16	4.85	5.22	5.42	5.75	5.71
Global productions of key compounds								
MVK	2.0	2.0	2.13	1.20	0.76	0.75	0.79	1.11
MACR	0.58	0.59	0.57	0.60	0.37	0.36	0.37	0.50
LISOPACOOH	0.60	0.58	0.74	0.61	0	0	0	0
ISOPBOOH	2.50	2.38	3.30	1.24	0.44	0.45	0.45	0.60
ISOPDOOH	0.59	0.58	0.67	0.63	0.19	0.19	0.18	0.24
ISOPEOOH	0	0	0	0	0.31	0.34	0.36	0.34
Isoprene nitrates	0.28	0.28	0.27	0.24	0.036	0.033	0.033	0.043
IEPOX	0	0	0	2.03	0.53	0.53	0.52	0.68
HPALD1	0	0	0	0	2.03	2.15	2.32	1.84
HPALD2	0	0	0	0	1.10	1.16	1.25	1.06

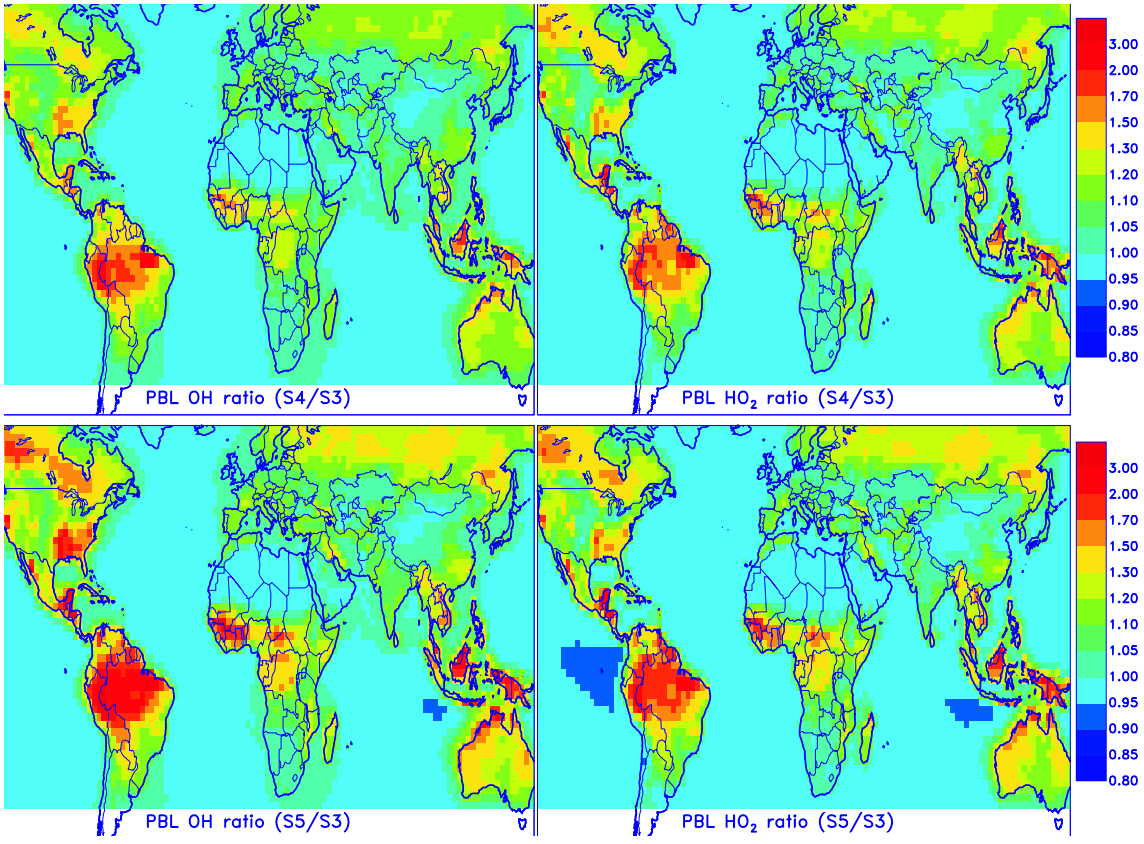

Fig. 4. Calculated impact on OH (left) and HO_2 (right) concentrations (July 2005, below 1.5 km) of the LIM0 mechanism update (Peeters et al., 2009; Peeters and Müller, 2010) with $m = 1$ (upper panels), and $m = 3$ (lower panels).

In spite of the large calculated impacts on HO_x, the LIM0 chemistry does not bring large changes in the calculated surface ozone, as shows the percentage change of surface ozone between the S3 and S5 simulations (Fig. 5). The moderate surface ozone increases over tropical regions (up to 8%) can be attributed to two main reasons. First, the much lower yield of isoprene nitrates in case S5 compared to S3 (Table 3) leads to a decreased loss of NO_x in the boundary

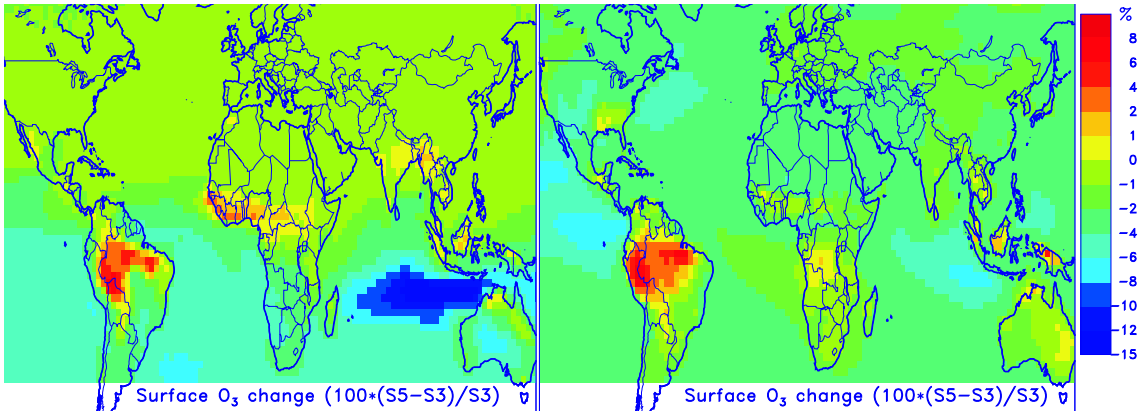

Fig. 5. Calculated impact on surface O_3 concentrations of the LIM0 mechanism update in January and July 2005.

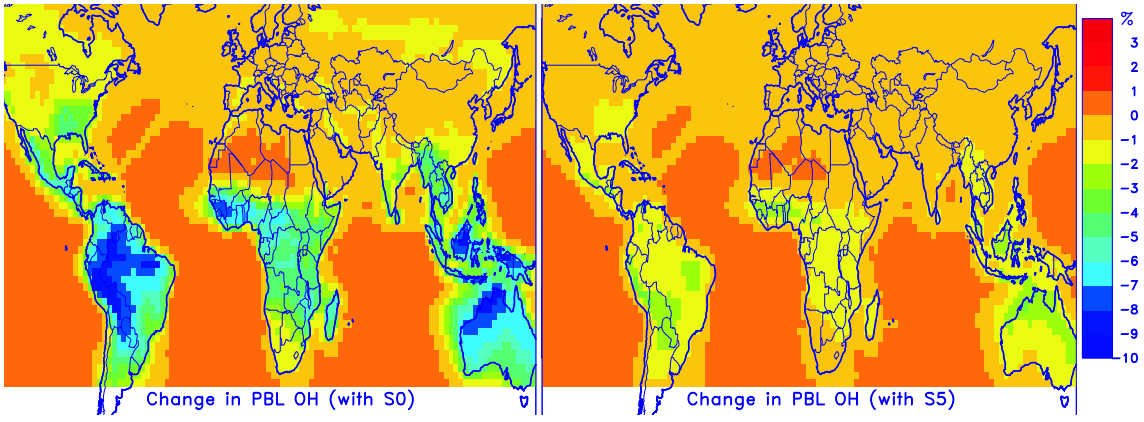

Fig. 6. Sensitivity of OH concentration to a 10% decrease of isoprene emissions using either the MIM2 mechanism (S0) or the LIM0 mechanism (S5).

layer over the emission regions, and thereby, to higher NO_x abundances and ozone chemical production rates. Second, as shown by sensitivity tests, the higher OH concentrations in the boundary layer in S5 reduces the relative contribution of the ozonolysis of alkenes to the removal of these compounds, resulting in a decreased ozone loss.

The calculated impact of the OH-regenerating epoxide formation and oxidation mechanism on OH concentrations is small but significant (up to 25%, Fig. 3). Nevertheless, the global epoxide formation, estimated to represent 42% of the total isoprene + OH sink in simulation S3 (240 Tg/yr), is strongly reduced when the LIM0 chemistry is introduced (10% or 62 Tg/yr in S5, 12% or 80 Tg/yr in S7). This reduction is caused by the competition of the 1,5- and 1,6-H shift reactions of the isoprene peroxys with their traditional bimolecular reactions, although this is partly compensated by the increased HO_2 concentrations. The decreased epoxide formation might have a large consequence on the modelled secondary organic aerosol (SOA) formation through this pathway (Paulot et al., 2009b). Further, accounting for the OH-formation channel in specific $RO_2 + HO_2$ reactions (S0 vs. S1) leads to only small increases in the boundary layer OH concentrations, by up to 6% over tropical forests compared to the S1 simulation, where this formation is neglected, whereas the changes in the HO_2 concentrations are even smaller (Fig. 2).

The artificial addition of OH radicals formed in the reactions of first generation isoprene peroxy radicals with HO_2 (MIM2+), proposed by Lelieveld et al. (2008), is tested in the S2 simulation. The impact of the hypothesized OH production has been explored in Butler et al. (2008), who studied the effect of adding $n = 1$, 2 or 3 extra OH radicals in these reactions, and concluded that the best match with the GABRIEL data was achieved for the $n = 2$, when the effective rate constant for isoprene oxidation by OH is taken equal to 50% of the lower bound of the IUPAC value range. In good agreement with the modelling results of Butler et al. (2008), the S2 simulation, which assumes $n = 2$, provides a significant increase of the OH concentrations in the boundary layer, by a factor of 1.5–2.5 over forested regions, compared to the S0 base case, as illustrated on Fig. 3, while much weaker changes are predicted for the corresponding

Table 4. Concentration of key compounds measured during the GABRIEL and INTEX-A campaigns and comparisons with the model simulations. The mean concentrations during daytime are used for the comparisons. The standard deviations are in parentheses.

	obs	S0	S1	S2	S3	S4	S5	S6	S7	S8
GABRIEL aircraft campaign, Suriname, October 2005 PBL, 9–17 LT (Lelieveld et al., 2008; Butler et al., 2008)										
OH (10^6 molec cm^{-3})	**5.6** (1.9)	1.06	1.05	2.45	1.22	2.6	4.08	4.11	3.65	3.38
HO_2 (10^8 molec cm^{-3})	**10.5** (2.7)	3.04	2.99	3.26	3.16	7.38	8.32	8.6	7.89	8.99
NO (pptv)	**20** (20)	23.7	24	12.5	25.1	21.8	18.2	18	18.3	14.5
C_5H_8 (ppbv)	**2.0** (0.76)	4.2	4.2	2.6	4.0	2.6	1.7	1.1	1.2	2.0
O_3 (ppbv)	**18.5** (4.6)	15.6	15.8	15.8	15.6	15.8	15.8	15.8	15.8	15.5
MACR + MVK (ppbv)	∼1	0.80	0.80	0.73	0.70	0.35	0.28	0.28	0.44	0.64
(MACR + MVK)/C_5H_8	∼0.5	0.19	0.19	0.28	0.17	0.13	0.16	0.25	0.36	0.32
INTEX-A aircraft campaign, Eastern US, July–August 2004, $z < 1$ km $[C_5H_8]_{PBL} > 0.3$ppbv, 9–17 LT (Ren et al., 2008)										
OH (10^6 molec cm^{-3})	**6.49** (1.5)	2.59	2.53	3.91	2.82	4.64	6.20	6.30	5.52	6.86
HO_2 (10^8 molec cm^{-3})	**9.86** (3.1)	5.72	5.6	6.36	5.71	8.77	9.65	9.95	9.19	7.55
NO (pptv)	**114** (130)	78	79	62	79	74	66	66	67	79
NO_2 (pptv)	**477** (460)	457	463	399	461	431	401	409	417	451
C_5H_8 (ppbv)	**0.94** (0.6)	6.40	6.48	4.67	6.11	4.23	3.21	2.06	2.37	0.94
O_3 (ppbv)	**53.3** (14)	55.3	55.3	55.8	55.1	54.1	53.9	54.9	55.4	54.1

HO_2 concentrations. Note that the precise value (0.5 or 0.9) of the reduction factor applied to the isoprene + OH rate is found to have little effect (< 5%) on HO_x concentrations in the boundary layer.

To summarize, the LIM0 chemistry, with a minor contribution of the epoxide formation mechanism, yields considerable enhancements in the boundary layer HO_x abundances over forested areas, reaching 50–300% for OH and 30–250% for HO_2 with respect to the MIM2 chemistry. Compared to the MIM2+ simulation, the enhancements reach 30–80% and 20–140% for OH and HO_2, respectively. The evaluation of these changes against selected campaign measurements is addressed in the next section.

3.2 Comparisons with observations

The modelled concentrations in the different simulations are compared with aircraft measurements from the GABRIEL and the INTEX-A campaigns.

The GABRIEL (Guyanas Atmosphere-Biosphere exchange and Radicals Intensive Experiment with the Learjet) campaign took place in October 2005 between 3°–6° N and 50°–60° W over the tropical Atlantic Ocean and the rainforests of Suriname and the Guyanas (Lelieveld et al., 2008). We compare the mean daytime GABRIEL measurements of OH, HO_2, NO, isoprene, and ozone concentrations, obtained over the Suriname tropical forest in the boundary layer, with the corresponding daytime (9–17 LT) modelled concentrations calculated within the region delimited by 3°–5° N and 52.5°–57.5° W and between 0 and 1.5 km (Table 4). We also compare the calculated sum of MACR and MVK abundances for each simulation with the PTR-MS observation obtained from Butler et al. (2008) and described in Eerdekens et al. (2009), as well as the (MACR + MVK)/isoprene ratio.

Measurements of OH, HO_2 and isoprene obtained from the NASA DC-8 aircraft during the Intercontinental Chemical Transport Experiment-A (INTEX-A) in July–August 2004 over North America and the western Atlantic Ocean are used for comparison with the model results. The data are accessible at the NASA Langley Research Center website (http://eosweb.larc.nasa.gov), and HO_x measurements are described in Ren et al. (2008). Note that the OH and HO_2 measured concentrations had to be multiplied by a factor of 1.64 to account for a calibration problem in the original dataset, as reported by Ren et al. (2008). Model and observation data shown in Table 4 are sampled at altitudes between 0 and 1 km during daytime (9–17 LT).

As seen on Table 4, a very good agreement is found between the GABRIEL measurements and the model simulations driven by the LIM0 chemistry, especially when the secondary OH regeneration in HPALD photolysis is taken into account (simulations S5–S8). In particular, the modelled OH concentrations, about 5 times too low compared to the observation when the MIM2 chemistry is used (S0) and about 2 times too low with the MIM2+ chemistry (S2), are only 30% lower in the S5/S6 simulations than the observed abundances. Equally important, the high observed HO_2 concentrations are reproduced within less than 30%, where the simulations using MIM2 chemistry fall short by a factor of 3.

Note that comparatively lower OH and HO_2 underestimations against these measurements were found by Butler et al. (2008) in calculations using the global model MESSy with the MIM2+ mechanism, and an isoprene + OH rate constant reduced by more than a factor of 2. This discrepancy with our results (simulation S2) can be at least partially explained by the factor of 2 overestimation of boundary layer ozone mixing ratios in Butler et al. (2008), leading to an overestimation of the primary source of HO_x by a similar factor. Other factors might contribute to differences in modelled HO_x concentrations, such as differences in the treatment of peroxy radical cross reactions, wet and dry deposition, boundary layer mixing, etc. As can be noted in Table 4, a very good agreement is obtained in IMAGESv2 for NO and ozone, providing confidence in the emission inventory used.

The average HO_2/OH ratio, equal to 190 in the observation, is best captured in S5–S6–S7 simulations (200–220), but is overestimated in S0 (290), and underestimated in S2 (133). The calculated isoprene boundary layer mean concentration is quite close to the measured values in the S5 simulation. The increased effective rate constant of the isoprene + OH reaction in the S6 simulation, leads to a stronger isoprene loss, and hence, to lower isoprene abundances in the boundary layer, from 1.7 in S5 to 1.1 ppbv in S6, consistent with the analysis of Butler et al. (2008) and Eerdekens et al. (2009). A sensitivity study (S8) conducted with an increased isoprene emission by 50% over Amazonia brings the model to a very good agreement with the measured isoprene abundances, with only little effect on the concentrations of OH (-7%) and HO_2 (+14%). The required increase in isoprene emissions is in apparent disagreement with conclusions by Ganzeveld et al. (2008) and Eerdekens et al. (2009), that the MEGAN isoprene fluxes should be roughly halved in order to match estimates based on isoprene and MACR + MVK concentration measurements. However, the MEGAN-derived average daytime (7–18 LT) isoprene flux used in IMAGESv2 simulations over the campaign area, about $4\,mg\,m^{-2}\,h^{-1}$ in early October, is well below the $6.9\,mg\,m^{-2}\,h^{-1}$ estimated by Eerdekens et al. (2009) based on measurements using a convective boundary layer (CBL) budgeting approach, therefore suggesting that the isoprene emission increase of simulation S8 is justified.

Halving the rate of the 1,6-H shift reactions (S7) results in only slightly (less than 10%) lower OH and HO_2 concentrations, nicely illustrating the strongly non-linear dependence of the impacts on the rate of these crucial reactions (Peeters and Müller, 2010). However, the MVK+MACR concentration is strongly enhanced in this simulation, bringing the (MVK+MACR)/isoprene in reasonable agreement with the observation (0.36 vs. ca. 0.5, Table 4).

We move now from the pristine rainforest to the more polluted conditions of the eastern US in summertime. The boundary layer HO_x concentrations measured during the INTEX-A campaign and simulated by the model are compared and illustrated in Figs. 7 and 8, while comparisons between mean modelled and observed daytime concentrations are summarized in Table 4. The S5 and S6 simulations provide an excellent agreement between the model and the HO_x measured concentrations in the boundary layer, as opposed to the underestimations found in the S0–S3 simulations, as well as in previously reported box modelling studies in the forested continental boundary layer (Ren et al., 2008). Changes in the segregation factor in S6, and in the 1,6-H shift reaction rate in S7 have a relatively small impact on the simulated HO_x mixing ratios. Nevertheless, the simulated isoprene mixing ratios over this region are found to be largely overestimated in comparison to the measurements, by a factor of 3 in the S5 case and by a factor of 2 in S6, most likely related to an overestimation of the isoprene emission in the MEGAN-ECMWF inventory used in the global model. This is in agreement with literature studies reporting that the isoprene emissions over the US might be significantly overestimated in the MEGAN inventory (Stavrakou et al., 2009b; Warneke et al., 2010). To evaluate the impact of lower isoprene emissions, we carried out a sensitivity study with halved isoprene emissions over the US (S8, Figs. 7, 8). In this case, the averaged modelled isoprene mixing ratio in the boundary layer matches the observation, while the OH concentration is by 10% higher than in the S5 case and the HO_2 concentration is decreased by 20%.

4 Conclusions

The IMAGESv2 CTM has been used to evaluate the impact of newly proposed pathways in the OH-oxidation of isoprene on HO_x abundances in the boundary layer. The tested mechanisms include (1) the traditional MIM2 chemistry (Taraborrelli et al., 2009), (2) the MIM2+ mechanism proposed by Lelieveld et al. (2008), (3) the epoxide formation pathways proposed by Paulot et al. (2009b), and (4) the LIM0 scheme proposed by Peeters et al. (2009) and Peeters and Müller (2010). We summarize below the main conclusions of this study.

1. The LIM0 scheme has a huge potential impact on HO_x concentrations over densely vegetated areas in the Tropics as well as at mid-latitudes. Modelled OH concentrations in the boundary layer are increased by a factor of about 4 over the Amazon basin, when using the LIM0 chemistry compared to the case where the MIM2 chemistry is used. The calculated impacts on HO_x are larger than those found with the artificial OH recycling proposed in the MIM2+ chemistry. Further, the simulated HO_2 concentrations are up to 2.5–3 times higher when using the LIM0 mechanism compared to the traditional schemes.

2. Hydroperoxy-aldehydes (HPALDs) are major products in the oxidation of isoprene by OH, with an average yield estimated to be about 60% on the global scale.

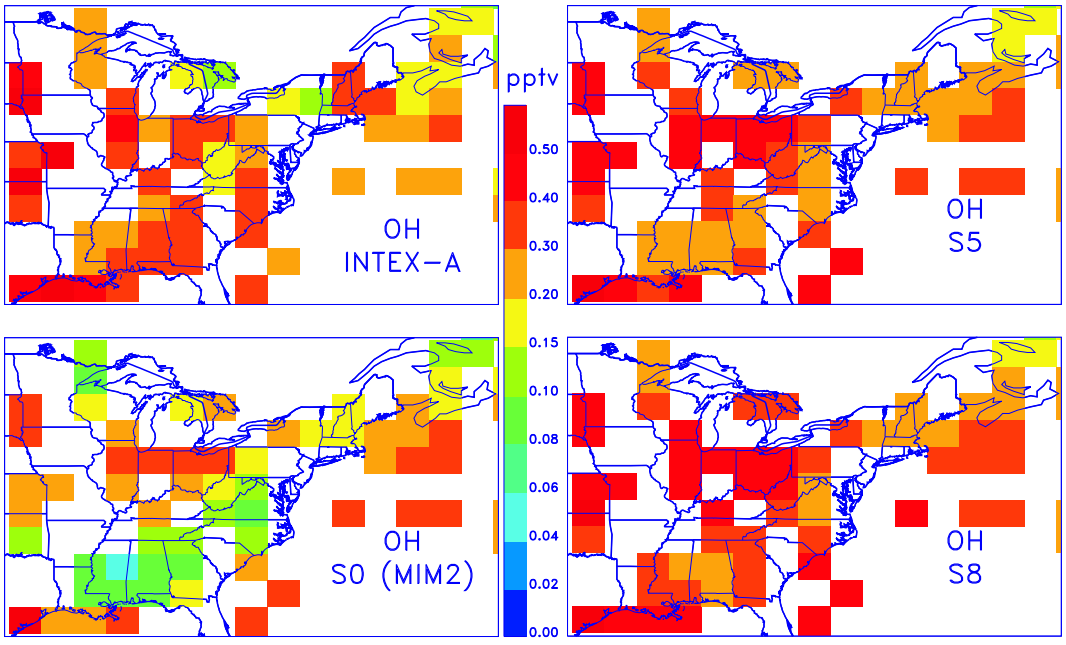

Fig. 7. Comparison of OH concentrations (below 1 km altitude, 9–17 LT average) measured during the INTEX-A campaign (top left), and modelled with IMAGESv2 using MIM2 (S0, bottom left), LIM0 (S5, top right), and LIM0 with halved isoprene emissions (S8, bottom right).

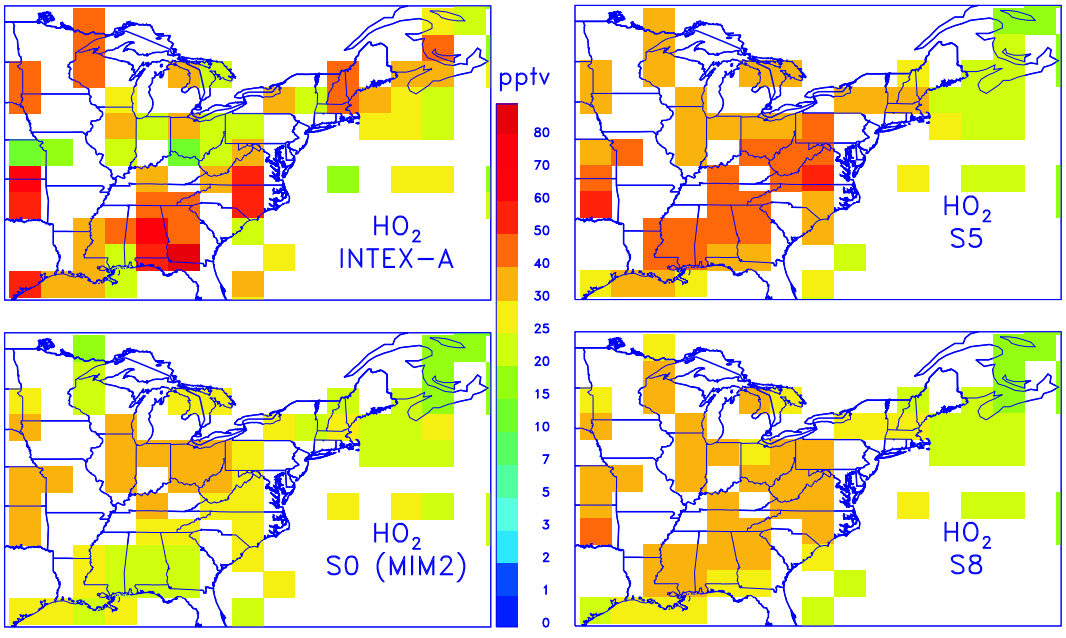

Fig. 8. Same as in Fig. 7 but for HO_2.

The globally averaged yield of MACR + MVK through the 1,5-H shift of Z-β-OH-peroxys from isoprene is estimated at ca. 10%. Reducing the 1,6-H shift rate estimate by a factor of 2 leads to only a small decrease of the globally averaged HPALD yield (50% instead of 60%) and to a significant increase (from 20% to 28%) of the total MACR + MVK yield.

3. The LIM0 chemistry brings the global model concentrations much closer to the observations used for validation than the other tested mechanisms. Our comparisons with the GABRIEL and INTEX-A measurements are very encouraging, as both OH and HO_2 observed mixing ratios in the boundary layer can be reproduced to within 30% – the measurement uncertainty – although

possible errors in the emissions and in the isoprene-OH segregation effect represent significant uncertainties.

4. A decrease of the isoprene emissions by about a factor of 2 over the Eastern US in the model is required in order to reproduce the isoprene measurements of the INTEX-A campaign. This finding is consistent with the reported overestimation in the MEGAN isoprene emissions by an independent analysis based on measurements from other aircraft campaigns over the US (Warneke et al., 2010).

5. Including the epoxide formation mechanism results in weak increases of the boundary layer OH concentrations (up to 25% when using MIM2 as reference mechanism, much less when LIM0 is introduced). Moreover, considering the OH-formation channel in the $RO_2 + HO_2$ reactions also brings small increases of the OH concentrations, by up to 6% in the Tropics.

6. The calculated surface ozone abundances are only slightly influenced by the use of the LIM0 chemistry in the global model, with increases of less than 10% over tropical forests.

It appears therefore that the newly proposed, theory-based LIM0 chemistry represents a major step towards a better understanding of the isoprene degradation chemistry in atmospheric conditions. However, large uncertainties still persist. Experimental confirmation and quantification is urgently needed for the formation of HPALDs and PACALDs, as well as for their fast OH-generating photolysis. Elucidating the further degradation of these major isoprene intermediates should therefore be a strong priority for future research.

Acknowledgements. The authors would like to thank the INTEX science team for making their data available. This research is partly funded by the Belgian Science Policy Office through the projects IBOOT (contract SD/AT/03, Science and Sustainable Development programme) and SECPEA (PRODEX), with additional support from FWO-Flanders and KULeuven Research Council.

Edited by: J. G. Murphy

References

Archibald, A. T., Cooke, M. C., Utembe, S. R., Shallcross, D. E., Derwent, R. G., and Jenkin, M. E.: Impacts of mechanistic changes on HO_x formation and recycling in the oxidation of isoprene, Atmos. Chem. Phys., 10, 8097–8118, doi:10.5194/acp-10-8097-2010, 2010.

Atkinson, R., Baulch, D. L., Cox, R. A., Crowley, J. N., Hampson, R. F., Hynes, R. G., Jenkin, M. E., Rossi, M. J., Troe, J., and IUPAC Subcommittee: Evaluated kinetic and photochemical data for atmospheric chemistry: Volume II - gas phase reactions of organic species, Atmos. Chem. Phys., 6, 3625–4055, doi:10.5194/acp-6-3625-2006, 2006.

Baeza-Romero, M. T., Glowacki, D. R., Blitz, M. A., Heard, D. E., Pilling, M. J., Rickard, A. R., and Seakins, P. W.: A combined experimental and theoretical study of the reaction between methylglyoxal and OH/OD radical: OH regeneration, Phys. Chem. Chem. Phys., 9(31), 4114–4128, doi:10.1039/b702916k, 2007.

Butkovskaya, N. I., Pouvesle, N., Kukui, A., and Le Bras, G.: Mechanism of the OH-initiated oxidation of glycolaldehyde over the temperature range 233–296 K, J. Phys. Chem. A, 110(50), 13492–13499, 2006a.

Butkovskaya N. I., Pouvesle, N., Kukui, A., Mu, Y., and Le Bras, G.: Mechanism of the OH-initiated oxidation of hydroxyacetone over the temperature range 236–298 K, J. Phys. Chem. A., 110(21), 6833–6843, 2006b.

Butler, T. M., Taraborrelli, D., Brühl, C., Fischer, H., Harder, H., Martinez, M., Williams, J., Lawrence, M. G., and Lelieveld, J.: Improved simulation of isoprene oxidation chemistry with the ECHAM5/MESSy chemistry-climate model: lessons from the GABRIEL airborne field campaign, Atmos. Chem. Phys., 8, 4529–4546, doi:10.5194/acp-8-4529-2008, 2008.

Dillon, T. J. and Crowley, J. N.: Direct detection of OH formation in the reactions of HO_2 with $CH_3C(O)O_2$ and other substituted peroxy radicals, Atmos. Chem. Phys., 8, 4877–4889, doi:10.5194/acp-8-4877-2008, 2008.

Eerdekens, G., Ganzeveld, L., Vilá-Guerau de Arellano, J., Klüpfel, T., Sinha, V., Yassaa, N., Williams, J., Harder, H., Kubistin, D., Martinez, M., and Lelieveld, J.: Flux estimates of isoprene, methanol and acetone from airborne PTR-MS measurements over the tropical rainforest during the GABRIEL 2005 campaign, Atmos. Chem. Phys., 9, 4207–4227, doi:10.5194/acp-9-4207-2009, 2009.

Ganzeveld, L., Eerdekens, G., Feig, G., Fischer, H., Harder, H., Königstedt, R., Kubistin, D., Martinez, M., Meixner, F. X., Scheeren, H. A., Sinha, V., Taraborrelli, D., Williams, J., Vilá-Guerau de Arellano, J., and Lelieveld, J.: Surface and boundary layer exchanges of volatile organic compounds, nitrogen oxides and ozone during the GABRIEL campaign, Atmos. Chem. Phys., 8, 6223–6243, doi:10.5194/acp-8-6223-2008, 2008.

Greenwald, E. E., Ghosh, B., Anderson, K. C., et al.: Isomer-selective study of the OH initiated oxidation of isoprene in the presence of O_2 and NO. I. The minor inner OH-addition channel, J. Phys. Chem., 114, 904–912, 2010.

Hofzumahaus, A., Rohrer, F., Lu, K., et al.: Amplified Trace Gas Removal in the Troposphere, Science, 324(5935), 1702–1704, doi: 10.1126/science.1164566, 2009.

Jenkin, M. E., Saunders, S. M., and Pilling, M. J.: The tropospheric degradation of volatile organic compounds: A protocol for mechanism development, Atmos. Environ., 31, 81–104, 1997.

Jenkin, M. E., Hurley, M. D., and Wallington, T. J.: Investigation of the radical product channel 20 of the $CH_3C(O)CH_2O_2 + HO_2$ reaction in the gas phase, Phys. Chem. Chem. Phys, 10(29), 4274–4280, 2008.

Karl, T.: Interactive comment on "Impacts of mechanistic changes on HO_x formation and recycling in the oxidation of isoprene" by A. T. Archibald et al., Atmos. Chem. Phys. Discuss., 10, C1699-C1702, 2010

Karl, M., Dorn, H.-P., Holland, F., Koppmann, R., Poppe, D., Rubb, R., Schaub, A., and Wahner, A. : Product study of the reaction of OH radicals with isoprene in the atmosphere simulation chamber SAPHIR, J. Atmos. Chem., 55, 167–187, 2006.

Karl, T., Guenther, A., Turnipseed, A., Tyndall, G., Artaxo, P., and Martin, S.: Rapid formation of isoprene photo-oxidation products observed in Amazonia, Atmos. Chem. Phys., 9, 7753–7767, doi:10.5194/acp-9-7753-2009, 2009.

Karl, T., Potosnak, M., Guenther, A., et al.: Exchange processes of volatile organic compounds above a tropical rain forest: Implications for modeling tropospheric chemistry above dense vegetation, J. Geophys. Res., 109, D18306, doi:10.1029/2004JD004738, 2004.

Krol, M., Molemaker, M., and de Arellano, J.: Effects of turbulence and heterogeneous emissions on photochemically active species in the convective boundary layer, J. Geophys. Res., 105, 6871–6884, 2000.

Kubistin, D., Harder, H., Martinez, M., Rudolf, M., Sander, R., Bozem, H., Eerdekens, G., Fischer, H., Gurk, C., Klüpfel, T., KÖnigstedt, R., Parchatka, U., Schiller, C. L., Stickler, A., Taraborrelli, D., Williams, J., and Lelieveld, J.: Hydroxyl radicals in the tropical troposphere over the Suriname rainforest: comparison of measurements with the box model MECCA, Atmos. Chem. Phys. Discuss., 8, 15239–15289, doi:10.5194/acpd-8-15239-2008, 2008.

Kuhn, U., Andreae, M. O., Ammann, C., Araùjo, A. C., Brancaleoni, E., Ciccioli, P., Dindorf, T., Frattoni, M., Gatti, L. V., Ganzeveld, L., Kruijt, B., Lelieveld, J., Lloyd, J., Meixner, F. X., Nobre, A. D., Pöschl, U., Spirig, C., Stefani, P., Thielmann, A., Valentini, R., and Kesselmeier, J.: Isoprene and monoterpene fluxes from Central Amazonian rainforest inferred from tower-based and airborne measurements, and implications on the atmospheric chemistry and the local carbon budget, Atmos. Chem. Phys., 7, 2855–2879, doi:10.5194/acp-7-2855-2007, 2007.

Lelieveld, J., Butler, T. M., Crowley, J. N., Dillon, T. J., Fischer, H., Ganzeveld, L., Harder, H., Lawrence, M. G., Martinez, M., Taraborrelli, D., and Williams, J.: Atmospheric oxidation capacity sustained by a tropical forest, Nature, 452, 737–740, 2008.

Martinez, M., Harder, H., Kubistin, D., Rudolf, M., Bozem, H., Eerdekens, G., Fischer, H., Klüpfel, T., Gurk, C., Königstedt, R., Parchatka, U., Schiller, C. L., Stickler, A., Williams, J., and Lelieveld, J.: Hydroxyl radicals in the tropical troposphere over the Suriname rainforest: airborne measurements, Atmos. Chem. Phys., 10, 3759–3773, doi:10.5194/acp-10-3759-2010, 2010.

Müller, J.-F. and Stavrakou, T.: Inversion of CO and NO_x emissions using the adjoint of the IMAGES model, Atmos. Chem. Phys., 5, 1157–1186, doi:10.5194/acp-5-1157-2005, 2005.

Müller, J.-F., Stavrakou, T., Wallens, S., De Smedt, I., Van Roozendael, M., Potosnak, M. J., Rinne, J., Munger, B., Goldstein, A., and Guenther, A. B.: Global isoprene emissions estimated using MEGAN, ECMWF analyses and a detailed canopy environment model, Atmos. Chem. Phys., 8, 1329–1341, doi:10.5194/acp-8-1329-2008, 2008.

Park, J., Jongsma, C. G., Zhang, R., and North, S. W.: OH/OD initiated oxidation of isoprene in the presence of O_2 and NO, J. Phys. Chem. A, 108, 10688–10697, 2004.

Paulot, F., Crounse, J. D., Kjaergaard, H. G., Kroll, J. H., Seinfeld, J. H., and Wennberg, P. O.: Isoprene photooxidation: new insights into the production of acids and organic nitrates, Atmos. Chem. Phys., 9, 1479–1501, doi:10.5194/acp-9-1479-2009, 2009.

Paulot, F., Crounse, J. D., Kjaergaard, H. G., Kürten, A., St. Clair, J. M., Seinfeld, J. H., and Wennberg, P. O.: Unexpected Epoxide Formation in the Gas-Phase Photooxidation of Isoprene, Science, 325, 730–733, doi:10.1126/science.11729102009, 2009b.

Peeters, J., Boullart, W., Pultau, V., Vandenberk, S., and Vereecken, L.: Structure-Activity Relationship for the addition of OH to (poly)alkenes: Site-specific and total rate constants, J. Phys. Chem. A, 111, 1618–1631, 2007.

Peeters, J., Nguyen, T. L., and Vereecken, L.: HO_x radical regeneration in the oxidation of isoprene, Phys. Chem. Chem. Phys., 11, 5935–5939, doi:10.1039/b908511d, 2009.

Peeters, J. and Müller, J.-F.: HO_x radical regeneration in isoprene oxidation via peroxy radical isomerisations, II: Experimental evidence and global impact, Phys. Chem. Chem. Phys., doi:10.1039/C0CP00811G, accepted, 2010.

Pugh, T. A. M., MacKenzie, A. R., Hewitt, C. N., Langford, B., Edwards, P. M., Furneaux, K. L., Heard, D. E., Hopkins, J. R., Jones, C. E., Karunaharan, A., Lee, J., Mills, G., Misztal, P., Moller, S., Monks, P. S., and Whalley, L. K.: Simulating atmospheric composition over a South-East Asian tropical rainforest: performance of a chemistry box model, Atmos. Chem. Phys., 10, 279–298, doi:10.5194/acp-10-279-2010, 2010.

Pugh, T. A. M., MacKenzie, A. R., Langford, B., Misztal, P. K., and Hewitt, C. N.: Estimating the segregation intensity of isoprene and OH over a South-East Asian tropical rainforest, Geophys. Res. Abstracts, 12, EGU2010–1914, EGU General Assembly, 2010b.

Ren, X., Olson, J. R., Crawford, J. H., et al.: HO_x chemistry during INTEX-A 2004: Observation, model calculation, and comparison with previous studies, J. Geophys. Res., 113, D05310, doi:10.1029/2007JD009166, 2008.

Sander, R. : Compilation of Henry's Law Constants for Inorganic and Organic Species of Potential Importance in Environmental Chemistry, version 3, 1999.

Sander, S. P., Finlayson-Pitts, B. J., Friedl, R. R., Golden, D. M., Huie, R. E., Keller-Rudek, H., Kolb, C. E., Kurylo, M. J., Molina, M. J., Moortgat, G. K., Orkin, L. V., Ravishankara, A. R., and Wine, P. H.: Chemical Kinetics and Photochemical data for use in atmospheric studies, Evaluation number 15, NASA Panel for data evaluation, JPL Publication 06-2, Jet Propulsion Laboratory, Pasadena, 2006.

Sandu, A. and Sander, R.: Technical note: Simulating chemical systems in Fortran90 and Matlab with the Kinetic PreProcessor KPP-2.1, Atmos. Chem. Phys., 6, 187–195, doi:10.5194/acp-6-187-2006, 2006.

Saunders, S. M., Jenkin, M. E., Derwent, R. G., and Pilling, M. J.: Protocol for the development of the Master Chemical Mechanism, MCM v3 (Part A): tropospheric degradation of non-aromatic volatile organic compounds, Atmos. Chem. Phys., 3, 161–180, doi:10.5194/acp-3-161-2003, 2003.

Spaulding, R. S., Schade, G. W., Goldstein, A. H., and Charles, M. J.: Characterization of secondary atmospheric photooxidation products: Evidence for biogenic and anthropogenic sources, J. Geophys. Res., 108(D8), 4247, doi:10.1029/2002JD002478, 2003.

A. F. Arellano Jr., Raeder, K., Anderson, J. L., Hess, P. G., Emmons, L. K., Edwards, D. P., Pfister, G. G., Campos, T. L., and Sachse, G. W.: Evaluating model performance of an ensemble-based chemical data assimilation system during INTEX-B field mission, Atmos. Chem. Phys., 7, 5695–5710, doi:10.5194/acp-7-5695-2007, 2007.

Stavrakou, T., MÜller, J.-F., De Smedt, I., Van Roozendael, M., Kanakidou, M., Vrekoussis, M., Wittrock, F., Richter, A., and Burrows, J. P.: The continental source of glyoxal estimated by the synergistic use of spaceborne measurements and inverse modelling, Atmos. Chem. Phys., 9, 8431–8446, doi:10.5194/acp-9-8431-2009, 2009.

Stavrakou, T., Müller, J.-F., De Smedt, I., Van Roozendael, M., van der Werf, G. R., Giglio, L., and Guenther, A.: Global emissions of non-methane hydrocarbons deduced from SCIAMACHY formaldehyde columns through 2003-2006, Atmos. Chem. Phys., 9, 3663–3679, doi:10.5194/acp-9-3663-2009, 2009.

Tan, D., Faloona, I., Simpas, J. B., Brune, W., Shepson, P. B., Couch, T. L., Sumner, A. L., Carroll, M. A., Thornberry, T., and Apel, E.: HO_x budgets in a deciduous forest: Results from the PROPHET summer 1998 campaign, J. Geophys. Res., 106(D20), 24407–24427, 2001.

Taraborrelli, D., Lawrence, M. G., Butler, T. M., Sander, R., and Lelieveld, J.: Mainz Isoprene Mechanism 2 (MIM2): an isoprene oxidation mechanism for regional and global atmospheric modelling, Atmos. Chem. Phys., 9, 2751–2777, doi:10.5194/acp-9-2751-2009, 2009.

van der Werf, G. R., Randerson, J. T., Giglio, L., Collatz, G. J., Kasibhatla, P. S., and Arellano Jr., A. F.: Interannual variability in global biomass burning emissions from 1997 to 2004, Atmos. Chem. Phys., 6, 3423–3441, doi:10.5194/acp-6-3423-2006, 2006.

Warneke, C., de Gouw, J. A., and del Negro, L., et al.: Biogenic emission measurement and inventories determination of biogenic emissions in the eastern United States and Texas and comparison with biogenic emission inventories, J. Geophys. Res., 115, D00F18, doi:10.1029/2009JD012445, 2010.

Wesely, M. L.: Parameterization of surface resistances to gaseous dry deposition in regional-scale numerical models, Atmos. Environ., 23, 1293–1304, 1989.